Technical note: Acidification methodology impacts sediment decarbonation as revealed by bulk and serial oxidation measurements

Songfan He[1], Huiyuan Yang[1], Xingqian Cui[1]

[1]School of Oceanography, Shanghai Jiao Tong University, Shanghai, 200030, China

5 *Correspondence to*: Xingqian Cui (cuixingqian@sjtu.edu.cn) or Huiyuan Yang (yhy_0707@sjtu.edu.cn)

Abstract. Acidification is frequently adopted to remove carbonates preceding particulate organic carbon (POC) measurements. In practice, acid rinsing and acid fumigation are two typical and well-established acidification methods eliminating inorganic carbon. However, detailed protocols therein are most likely adopted based on conventional laboratory practices, assuming that the measurement precision is unaffected by experiment conditions. In fact, acidification can cause mineral dissolution and

10 leaching of organic components, and therefore impacts the quantity and composition of residual POC considerably. Nonetheless, the effect of acidification on POC properties and the underlying mechanisms are ambiguous when relying solely on bulk measurements. In this study, we investigated POC properties following acidification using ramped temperature pyrolysis/oxidation (RPO) technique, in combination with bulk carbon analyses, to assess the impact of different decarbonation pretreatments on the sedimentary organic carbon (OC) measurements. Our results reveal that both acidification method (rinsing

15 or fumigation) and HCl concentrations under acid rinsing are main factors dictating OC properties measured. Notably, despite negligible differences in bulk measurements, RPO results show distinct variations between these two acidification methods. In combination with other evidence, our study suggests that the alteration of organic-inorganic associations, which is ubiquitous during acidification, drives the behaviour of POC properties that measured. Furthermore, we demonstrate that the characteristics of residual POC in acid-rinsed samples are more proximal to pristine, natural states of the raw materials, whereas

20 the strikingly discrepant differences between two acidification methods can be attributed mainly to the perturbation caused by calcium chlorides after acid fumigation.

1 Introduction

Geochemical proxies are extensively utilized to expand our understanding of natural processes in modern environments and over geological time scales. Total organic carbon (TOC) content and stable carbon isotope (δ^{13}C) of TOC, two simple and

25 essential proxies therein, are critical in quantitative estimates. Numerous studies leveraged TOC and several environmental variables (e.g., denudation rates, sedimentation rates and water discharge) to constrain regional and global carbon fluxes (Dellinger et al., 2023; Smith et al., 2015; Hage et al., 2022; Zondervan et al., 2023); whereas δ^{13}C signatures are critical in discriminating sources of organic carbon (OC) (e.g., terrestrial or marine) or unraveling biological synthetic pathways (Berg et al., 2010; Meyers and Ishiwatari, 1993). Therefore, accurate measurements of above proxies are the premise of data

30 interpretations. Current instrument advancing allows us to acquire relatively accurate data, with precisions of < 0.1% for TOC
and < 0.1‰ for $\delta^{13}C$. However, artificially-induced methodological biases, while being frequently ignored, introduce
considerable and potentially more significant variations to the results. This is largely due to conventional adoption of different
laboratory-based sample pretreatment methods.

Prior to TOC and $\delta^{13}C$ measurements, the inorganic carbon is removed using acidification. Typical methods include direct

35 addition of hydrochloric acid (HCl) solution to particulates in the aqueous phase followed by subsequent rinses with Milli-Q
water (i.e., acid rinsing) and acidification by exposure to acid in the vaporous phase (i.e., acid fumigation). Moreover, acid
rinsing may vary in concentrations of HCl being applied, whereas acid fumigation in some cases is followed by water rinsing
to remove chlorides in recent studies (Hemingway et al., 2017a). These various acidification pretreatments can yield diverse
impacts on OC compositions (Brodie et al., 2011; Komada et al., 2008; Lohse et al., 2000). Specifically, acid rinsing might

40 lead to OC dissolution/hydrolysis (Galy et al., 2007; Schmidt and Gleixner, 2005), whereas acid fumigation is speculated to
alter organo-mineral interactions (Plante et al., 2013) and is unsuitable for samples rich in carbonates (Hedges and Stern, 1984).
Additionally, freeze-drying versus oven drying and the temperatures selected for the latter may result in further uncertainties
(Mcclymont et al., 2007).

For decades, several studies compared the effect of acidification on OC analysis; however, the nuanced results remain

45 inconsistent or even contradictory (Brodie et al., 2011). The contentious results are somewhat conceivable, since natural
samples are a mixture of compounds and bulk OC data is the superposition of myriad signals. In comparison with bulk
measurements, the recently developed ramped-temperature pyrolysis/oxidation technique has the advantage to interpret total
OC as a reactive continuum and thus separate different signals. The RPO analysis progressively converts organic carbon to
CO_2 throughout a continuous heating process (Cui et al., 2022; Hemingway et al., 2017a; Rosenheim et al., 2008).

50 Thermochemically labile OC is prone to decompose at early heating stage, whereas refractory OC converts to CO_2 at higher
temperatures. Thus, OC of different sources (e.g., biogenic OC, rock-derived OC) within samples can be, in part, discriminated
in RPO analyses. This offers a window to "unfold" bulk C data to two-dimensional configurations characterized by OC species
with relative quantities.

In this study, we systematically conducted a suite of contrasting experiments with various, aforementioned pretreatment

55 conditions, including different acidification methods (rinsing vs. fumigation), concentrations of hydrochloric acid (1 N, 2 N, 4
N, 6 N and 12 N for fumigation), reaction durations (6 h, 12 h and 24 h), drying methods (freeze-drying vs. oven drying), the
temperature for oven drying (45 °C vs. 60 °C), and the temperature for reaction (ambient vs. 60 °C). All samples were subject
to bulk and RPO measurements, of which the latter is used to decipher the methodological impacts on OC quantities and
compositions. Apart from traditional criteria (e.g., the effectiveness of IC removal), we assessed the potential modification of

60 chemical structures within samples induced by acidification pretreatments as another line of criterion in assessing the
applicability of an acidification method. Finally, we summarize the likely influence of different pretreatment conditions and
further offer optimal suggestions for acidification.

2 Materials and methods

2.1 Samples and preparation

[handwritten annotation: Why use complex Names for samples? maybe simple would be easier for reader "Eocene rock" "permian rock" "modern estuary sediment" "modern fjord sediment" or similar]

65 Four samples with different properties were selected, including two lithified ancient sediments and two modern sediments. These samples were collected, respectively, from: (i) the Eocene Green River Formation (sedimentary rock, termed "1207-GR-11"); (ii) the Permian-Triassic Meishan section (sedimentary rock, termed "MS05-135"); (iii) the Yangtze River Estuary (modern sediment, termed "CJK A6-3"); and (iv) Isfjorden fjord of Svalbard (modern sediment, termed "AREX R7"). Two rock samples (i.e., 1207-GR-11 and MS05-135) have similar TOC values but contrasting carbonate contents, whereas the other

70 two surface sediment samples (i.e., CJK A6-3 and AREX R7) are differentiated by TOC values, but are similar in carbonate contents. All these samples were grounded into powder, homogenized, and divided into 13 aliquots, respectively, for subsequent processing.

2.2 Experimental design and operations

[handwritten annotation: Maybe specify what "EC" means – "experimental conditions"?]

We conducted two approaches of acidification, i.e. acid rinsing (EC-1 to EC-10) and acid fumigation (EC-11 and EC-12). *[handwritten annotation: table 1]*

75 Particularly, samples of acid rinsing were pretreated with various conditions to compare the influence of HCl concentrations (EC-1, EC-2, EC-3 and EC-4), acidification durations (EC-1, EC-5 and EC-6), drying methods and temperatures (EC-1, EC-7 and EC-8), the potential influence of heating at decarbonation reactions (EC-1 and EC-9) and prolonged exposure to concentrated acid (EC-10). Additionally, acid fumigation methods (EC-11 and EC-12) were carried out to compare with acid rinsing and to examine the effect of water rinsing following acid fumigation (Bao et al., 2019; Harris et al., 2001; Hemingway

80 et al., 2017a). For clarity purpose, we particularly termed EC-11 and EC-12 as "fume I" and "fume II", respectively.

Each set of 12 aliquots were first acidified, where 10 were treated with acid rinsing method and two with acid fumigation *[handwritten annotation: repeat of above?]* (Table 1). For acid rinsing, each aliquot (> 200 mg) was weighed in a 50 mL glass centrifuge tube, followed by the addition of HCl with a specific concentration (i.e., 1 N, 2 N, 4 N or 6 N). To ensure that IC was completely removed, we gradually added HCl in excess. Moreover, we stirred solid-liquid mixtures during and after acidification using a portable vortex mixer.

85 To investigate the effect of heating, one aliquot was maintained at 60 °C (± 3 °C) for 1 h after acidification. All centrifuge tubes were left for 6 h, 12 h, or 24 h according to designated experimental conditions (see Table 1). Afterwards, the supernatants were removed using pipettes after centrifugation and the residual solids were rinsed with Milli-Q water for three to four times to be neutralized.

For fumigation method (EC-11, EC-12), eight subsamples were weighed and placed in a glass petri dish (Φ 60 mm × 35 mm). *[handwritten annotation: added]*

90 Before fumigation, we carefully instilled several drops of Milli-Q water into each subsample to form a thin film of water on the surface (Harris et al., 2001; Yamamuro and Kayanne, 1995). Eight subsamples were then placed into a bilayer glass desiccator together with a glass beaker of ~50 mL 12 N HCl at the bottom. All subsamples were then exposed to acid vapors at room temperature for 12 h. After fumigation, subsamples were supplied with two additional drops of aqueous HCl to verify

Table 1. Combinations of experimental conditions in this study, including acidification methods, HCl concentrations, reaction
95 durations and temperature, as well as drying methods and temperature.

Experimental conditions					
Acidification method	HCl concentration	Reaction temperature	Duration	Drying method	Mark*
Rinsing	1 N	Ambient	12 h	Freeze-drying	EC-1
Rinsing	2 N	Ambient	12 h	Freeze-drying	EC-2
Rinsing	4 N	Ambient	12 h	Freeze-drying	EC-3
Rinsing	6 N	Ambient	12 h	Freeze-drying	EC-4
Rinsing	1 N	Ambient	6 h	Freeze-drying	EC-5
Rinsing	1 N	Ambient	24 h	Freeze-drying	EC-6
Rinsing	1 N	Ambient	12 h	Oven drying, 45°C	EC-7
Rinsing	1 N	Ambient	12 h	Oven drying, 60°C	EC-8
Rinsing	1 N	60°C#	12 h	Freeze-drying	EC-9
Rinsing	6 N	Ambient	24 h	Freeze-drying	EC-10
Fumigation + Rinsing	12 N	Ambient	12 h	Freeze-drying	EC-11
Fumigation	12 N	Ambient	12 h	Oven drying, 60°C	EC-12

*"EC" is the abbreviation of "experimental condition", and the suffixal numbers are for sorting purpose.
#60°C water bath for the first hour, and then retained at room temperature.

the effectiveness of decarbonation. This is based on the former practice that acid fumigation is not suitable for samples
100 containing a great portion of CaCO$_3$ (Hedges and Stern, 1984). As expected, two subsamples of 1207-GR-11 containing ~ 70%
w/w CaCO$_3$ bubbled violently, indicating residual carbonate, whereas the others show no visible reaction. We then added HCl
in excess to completely remove unreacted CaCO$_3$ in 1207-GR-11 subsamples. Afterwards, four EC-11 subsamples therein
were additionally rinsed with Milli-Q water for three times prior to freeze-drying.

Air drying, oven drying and freeze-drying are typical drying methods, with the latter two being compared in this study. The
105 majority of subsamples were freeze-dried at 60 °C for more than 24 h while other subsamples were dried in oven at 45 °C or
60 °C for ~ 40 h (Table 1). Two different temperatures were adopted to examine possible influence of oven drying temperatures.
Fumigated subsamples were dried at 60 °C due to the concern that 45 °C was likely impotent to remove acid vapors completely,
and thus corrode instruments. To minimize the corrosive effect of vaporized HCl, fumigation subsamples (those dried by oven)
were oven dried aside with sodium hydroxide flakes. After drying, subsamples were homogenized with an agate mortar and
110 pestle. All glass containers were pre-combusted at 550 °C for 6 h to eliminate contaminants.

2.3 Bulk carbon measurement

Each homogenized carbonate-free subsample was divided into two aliquots for bulk and RPO analyses (see Sect. 2.4), respectively. For bulk carbon measurement, an aliquot containing ~200 µg OC was weighed, placed and wrapped in a tin capsule. Sample-containing tin capsules were transferred into the autosampler of a Thermo Fisher Scientific Flash IRMS

115   elemental analyzer (EA) coupled to an Electron DELTA V Advantage isotope ratio mass spectrometer (IRMS). The resulting TOC and $\delta^{13}C$ values (Table 2) were then calibrated using three standards (i.e., USGS 40, USGS 62, USGS 64). The standard deviations (SDs) of TOC and $\delta^{13}C$ were 0.7% (relative) and 0.06‰ (absolute) based on USGS 40 (n = 5).

Table 2. Bulk and RPO parameters of all subsamples. Bulk parameters include TOC and $\delta^{13}C$; RPO parameters include the average activation energy (μ_E), the standard deviation of activation energy (σ_E), the fractions of OC with activation energy

120   lower than 150 kJ mol^{-1} ($f_{E<150}$) and lying within 150-185 kJ mol^{-1} ($f_{150\leq E<185}$). Carbonate contents are included as well. Each row stands for a subsample subjected to a specific experimental condition. N. A. indicates not applicable.

Sample ID	Pretreat-ment	Carbonate (%)	Bulk		RPO			
			TOC (%)	$\delta^{13}C$ (VPDB, ‰)	μ_E (kJ mol^{-1})	σ_E (kJ mol^{-1})	$f_{E<150}$	$f_{150\leq E<185}$
1207-GR-11	EC-1	68.4	0.525	-28.95	188.51	22.97	0.046	0.309
1207-GR-11	EC-2	69.5	0.519	-29.26	188.89	23.50	0.047	0.306
1207-GR-11	EC-3	70.3	0.519	-28.90	188.91	24.16	0.051	0.307
1207-GR-11	EC-4	70.5	0.520	-29.27	189.13	24.94	0.059	0.304
1207-GR-11	EC-5	68.7	0.525	-28.95	191.46	23.30	0.040	0.270
1207-GR-11	EC-6	68.5	0.522	-29.04	188.01	22.66	0.047	0.311
1207-GR-11	EC-7	68.3	0.532	-28.94	189.40	22.88	0.045	0.296
1207-GR-11	EC-8	69.1	0.521	-29.01	189.73	22.72	0.044	0.291
1207-GR-11	EC-9	68.4	0.535	-28.96	187.83	22.95	0.048	0.316
1207-GR-11	EC-10	70.2	0.533	-29.03	186.58	24.26	0.064	0.324
1207-GR-11	EC-11	71.6	0.482	-29.03	188.08	24.54	0.058	0.313
1207-GR-11	EC-12	N. A.	0.518	-28.94	165.85	19.41	0.174	0.705
MS05-135	EC-1	8.8	0.586	-24.48	204.40	21.33	0.016	0.135
MS05-135	EC-2	10.0	0.610	-24.46	203.94	21.27	0.015	0.138
MS05-135	EC-3	11.0	0.597	-24.27	202.81	22.03	0.019	0.127
MS05-135	EC-4	11.5	0.604	-24.15	197.39	23.47	0.025	0.243
MS05-135	EC-5	7.7	0.584	-24.22	203.73	21.64	0.018	0.132
MS05-135	EC-6	10.0	0.607	-24.43	205.10	22.19	0.019	0.129
MS05-135	EC-7	8.4	0.580	-24.41	205.48	22.28	0.019	0.128

MS05-135	EC-8	8.9	0.596	-24.49	202.89	21.71	0.020	0.141
MS05-135	EC-9	10.7	0.596	-24.37	204.54	22.39	0.019	0.125
MS05-135	EC-10	11.6	0.604	-24.57	194.20	25.11	0.034	0.297
MS05-135	EC-11	12.8	0.587	-24.65	193.54	23.57	0.034	0.284
MS05-135	EC-12	N. A.	0.568	-24.51	180.33	24.71	0.059	0.581
CJK A6-3	EC-1	13.7	0.395	-22.82	175.58	35.14	0.205	0.447
CJK A6-3	EC-2	14.5	0.388	-23.09	175.47	35.25	0.205	0.443
CJK A6-3	EC-3	16.4	0.387	-22.90	176.48	35.33	0.192	0.438
CJK A6-3	EC-4	17.7	0.373	-23.08	177.18	35.55	0.186	0.443
CJK A6-3	EC-5	13.4	0.408	-23.09	175.54	35.28	0.206	0.444
CJK A6-3	EC-6	14.5	0.394	-22.77	177.36	35.23	0.194	0.430
CJK A6-3	EC-7	13.2	0.398	-22.66	175.35	35.71	0.220	0.435
CJK A6-3	EC-8	13.4	0.408	-22.80	174.56	35.58	0.230	0.432
CJK A6-3	EC-9	15.3	0.397	-22.88	177.39	35.15	0.189	0.432
CJK A6-3	EC-10	18.3	0.385	-23.30	178.32	35.22	0.173	0.445
CJK A6-3	EC-11	16.8	0.402	-22.99	175.82	34.95	0.198	0.444
CJK A6-3	EC-12	N. A.	0.440	-23.31	169.29	32.61	0.293	0.388
AREX R7	EC-1	13.8	1.224	-26.84	188.64	26.88	0.088	0.269
AREX R7	EC-2	15.0	1.153	-26.85	188.38	26.25	0.083	0.267
AREX R7	EC-3	17.2	1.131	-27.16	187.51	25.61	0.069	0.323
AREX R7	EC-4	18.3	1.144	-27.03	182.93	26.08	0.083	0.425
AREX R7	EC-5	13.2	1.210	-26.89	189.99	26.59	0.085	0.244
AREX R7	EC-6	14.6	1.147	-26.80	190.39	26.33	0.079	0.240
AREX R7	EC-7	13.2	1.175	-27.12	187.66	26.94	0.095	0.289
AREX R7	EC-8	13.6	1.152	-26.92	187.60	27.02	0.096	0.291
AREX R7	EC-9	15.5	1.179	-27.20	189.16	26.12	0.075	0.263
AREX R7	EC-10	17.7	1.182	-26.84	183.56	26.23	0.082	0.418
AREX R7	EC-11	20.9	1.128	-27.13	180.57	25.71	0.097	0.461
AREX R7	EC-12	N. A.	1.230	-26.87	183.41	30.45	0.111	0.449

Did EC-12 remove all carbonate?

2.4 RPO analysis

The integrated RPO system utilized here is primarily comprised of a carrier gas unit, a programmable pyrolysis furnace and
125   an infrared CO_2 analyzer. The pyrolysis furnace consists of two insulated furnaces (i.e., the upper and the lower) with

An image or drawing of RPO system would be useful

thermocouples equipped. A large quartz tube was inserted into the middle chamber of furnaces with catalytic wires mounted in the lower half. During each RPO run, a smaller-sized quartz reactor with an aliquot containing ~1 mg OC at its bottom was introduced into the upper half of the large quartz tube. Afterwards, the upper furnace was heated at a constant ramping rate of 5 °C min⁻¹ from ~ 60 °C to > 1000 °C with steady carrier gas flow rate, whereas the lower furnace was maintained isothermally

130   at 800 °C. The carrier gas flow in the inner quartz tube was 27 mL min⁻¹ of helium mixed with 3 mL min⁻¹ diluted oxygen (5% oxygen). This sub-oxidation mode was consistently adopted in this study to circumvent possible charring during heating (Huang et al., 2023; Stoner et al., 2023). Further, additional 5 mL min⁻¹ pure oxygen was introduced to the interface of two furnaces to completely oxidize vaporized OC fragments downstream. For blank control, quartz tubes were combusted at 1000 °C for ~ 8h prior to RPO analyses. Generally, the precision of the ramping temperature rate was < 0.2%; whereas evolved CO_2

135   concentrations were calibrated against standard gas containing 2000 ppm CO_2.

We also noted that the residual chloride may generate chlorine gas under ramping temperatures. The chlorine gas further reacts with catalytic wires, and thus, distorts the authenticity of thermograms (Hemingway et al., 2017b; Huang et al., 2023). This consideration was of no concern to acid rinsing aliquots as the majority of chloride ions were removed after repeated rinses and dilution, whereas considerable amount of chloride in acid fumigation counterparts, especially those dried by oven, surged

140   the risk. To continuously track the status of catalytic wires, we ran an in-house sample (termed "Irati T2") as the standard, under the same conditions (ramped rate, carrier gas flow rate and O_2 concentration), before and after RPO analysis of those fumigation-treated, oven-dried aliquots. The RPO results of standard samples are presented in the supplementary file (Fig. S1).

2.5 Data analysis

Based on the initial experimental design, we determine EC-1 as the control groups to simplify our calculation of relative

145   variations of bulk results. However, we clarify that the determination of a particular group as the control does not change or bias our calculation of variables and thus conclusions drawn. For convenience, we number the four samples from 1 to 4, following the same order in Table 2, and sort subsamples by the order from 1 to 12 according to pretreatment procedures. Then, we can quantify the relative changes of bulk TOC in our sample set as

$$\Delta(TOC)_{i,j} = \frac{TOC_{i,j} - TOC_i^*}{TOC_i^*}, i = 1, ..., 4, j = 2, ..., 12,$$ (1)

150   where $TOC_{i,j}$ is the TOC value of the i-th sample treated by the j-th experimental condition (i.e., EC-j) and TOC_i^* is the TOC value of the i-th sample with control conditions (i.e., EC-1). Note that the results derived from Eq. (1) are relative changes, offsetting the discrepancies between samples with variable TOC values. Similarly, we can derive the changes of $\delta^{13}C$ signatures as

$$\Delta(\delta^{13}C)_{i,j} = \delta^{13}C_{i,j} - \delta^{13}C_i^*, i = 1, ..., 4, j = 2, ..., 12,$$ (2)

155 noting that it is the absolute form, which is different from Eq. (1). The results derived from Eqs. (1) and (2) are either positive or negative, corresponding to enrichment or depletion, respectively, relative to the control groups.

RPO analyses and the generation of thermograms were conducted for all acidified aliquots and homogenized raw materials. RPO thermograms were further converted to probability density distributions (i.e, $p[E]$) by the inverse method (Hemingway et al., 2017a), following an open-source package "rampedpyrox" in Python (Hemingway, 2016). Three fundamental

160 parameters, including the mean value of E (termed "μ_E"), the standard deviation of E (termed "σ_E"), and the proportion of OC within the range of E from a kJ mol^{-1} to b kJ mol^{-1} (termed "$f_{a<E<b}$"), were calculated for statistic analyses. The default value of the lower bound "a" is 50 kJ mol^{-1}, if not specified.

The mean of E was calculated as:

$$\mu_E = \int_0^\infty E p(E) dE \tag{3}$$

165 The square root of the variance of E was calculated as:

$$\sigma_E = (\mu_{E^2} - [\mu_E]^2)^{1/2} \tag{4}$$

The proportion of OC within a specific E range (a kJ mol^{-1} to b kJ mol^{-1}) was calculated as:

$$f_{a<E<b} = \int_a^b p(E) dE \tag{5}$$

RPO parameters measured and/or calculated as well as bulk parameters of all subsamples are listed in Table 2. Based on RPO

170 results of the in-house standard (n=8), the standard deviation (SD) of μ_E is 0.50 kJ mol^{-1}, and SD of σ_E is 0.18 kJ mol^{-1}, denoting excellent reproducibility.

3 Results and discussion

3.1 A snapshot of the influence from each factor on bulk parameters

Compared with the control groups, most TOC and δ^{13}C results exhibit marginal fluctuations within a range of ± 5% and ±

175 0.4‰, respectively (Fig. 1). It should be noticed that none of the factors exert an unambiguous control on bulk results. To better grasp net effects of each factor, we arithmetically averaged deviations of four samples under each condition (Fig. 1). Enhanced loss of OC is observed under elevated concentrations of HCl (1 N to 6 N) (Fig. 1b). The consistent depletion of δ^{13}C signatures with 2 N to 6 N HCl in relative to control conditions (1 N) indicates preferential loss of ^{13}C-enriched moieties. It was recognized that hydrolysable OC (e.g., amino acids), in general, are enriched in ^{13}C relative to bulk average and the acid-

180 insoluble counterpart (Hwang and Druffel, 2003; Wang et al., 1998). Thus, we speculate that lower bulk δ^{13}C signatures after acid rinsing are attributed to the preferential loss of hydrolysable OC. Such observation is further corroborated by stronger loss of OC and larger offsets of δ^{13}C values of EC-11 (fume I), which was fumigated with 12 N HCl and rinsed afterwards with

Milli-Q water. It suggests that a greater proportion of sedimentary OC is possibly hydrolyzed under concentrated HCl and further washed away (Fig. 1b) (Bao et al., 2019; Brodie et al., 2011).

order not consistent with table 1 →

Not clear

185

"Mart" → EC-2

10? 3 4 11 12 5 6 7 8 9 ?
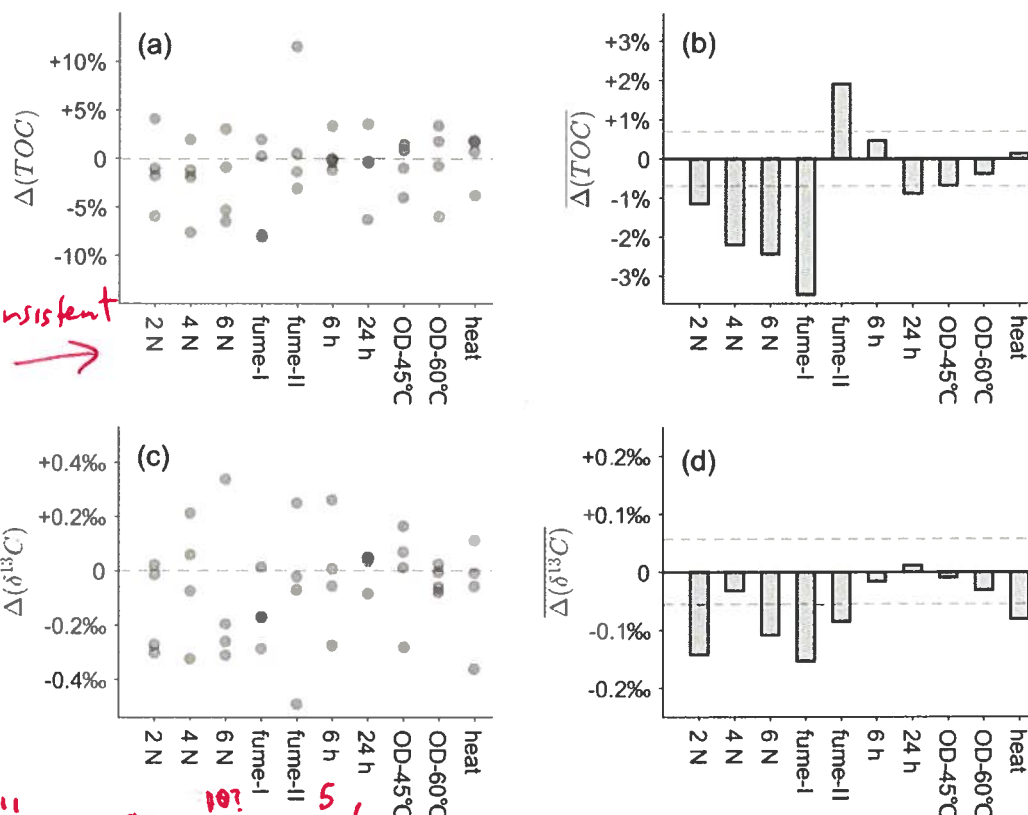
Fig 1: An integrated assessment of influence of all factors on bulk parameters. **(a)** and **(c)** exhibit deviations of each experiment from the control groups (EC-1) at the sample level. The control groups (EC-1) are not included, whereas each grey dot represents one subsample after a particular pretreatment. The datum lines (dash lines) in **(a)** and **(c)** are reference values of TOC and δ^{13}C. Grey dots above and below the datum lines indicate relative enrichment or depletion, respectively. To delineate

190 the net effects of all factors, bar plots of the average deviations (i.e., the mean value of four grey dots in vertical) are correspondingly plotted in **(b)** and **(d)**. The dash lines in **(b)** and **(d)** are standard deviations in measurements of TOC ($\pm0.7\%$) and δ^{13}C ($\pm0.056\permil$), respectively.

In contrast, EC-12 (fume II) without water rinsing exhibits higher TOC contents than samples with water rinsing, suggestive *EC-12*

195 of efficient retention of labile components that are hydrolyzed and dissolvable. Surprisingly, the TOC contents of fume II — offset the most with that of fume I and are even higher than those of samples under control conditions. It implies that the

ackward

control condition as defined in this study may still lead to the loss of a proportion of labile, dissolvable OC, rendering former postulations (Huang et al., 2023). However, despite mitigated OC loss on average, some fume II subsamples exhibit slightly lower TOC values than those under the control condition (Fig. 1a), presumably attributed to volatilization of labile materials

200   during the oven drying process (Bisutti et al., 2004; Caughey et al., 1995).

Other experimental conditions, including the reaction time, drying method and reaction temperature show inconspicuous *small* changes in TOC and $\delta^{13}C$ values. In fact, most values are close to or within ranges of standard deviations (Fig. 1), indicative *indicating* of their limited influence on bulk parameters. However, we noticed that prolonged reaction and oven drying process slightly promote OC loss, whereas heating makes no difference (Fig. 1).

205   Overall, acid fumigation versus acid rinsing and HCl concentrations for the latter are two key factors to consider for *Isotopic influence* acidification conditions, whereas other factors exert minimal effects on bulk *TOC* results. Conceivably, this is likely also the case for their influence on thermographic *? Heating ?* properties. In the next section, we continue to decipher the mechanisms of discrepant TOC and $\delta^{13}C$ values caused by these two key factors based on the thermochemical analysis.

influence on
3.2 HCl concentration biases thermochemical properties and potential mechanisms

Spell out at start of new section (remind reader)
210   RPO results show that samples after acidification, whether by fumigation or rinsing, exhibit pronounced deviations in thermograms and energy distributions, which are more prominent than results recorded by bulk parameters (TOC and $\delta^{13}C$). In terms of subsamples treated by acid rinsing, changes in secondary factors (e.g., reaction time, drying methods and temperatures) exert insignificant or erratic influence on the distribution patterns of thermograms (Supplementary file Fig. S2 and S3). In contrast, almost all the thermographic patterns show definitely systematic gradation along the gradient of HCl

215   concentrations (Fig. 2).

To reconcile and depict coincident variations of thermograms and HCl concentrations, we orthogonally decompose evolutionary trends of thermograms into two directions. Changes in the vertical orientation are interpreted as enrichment or loss of OC, whereas horizontal shifts represent alterations in thermal stability and, presumably, structural distortion. Intriguingly, all four samples in this study exhibit distinct patterns encompassing different vertical and horizontal variations.

220   Notably, the intensity of OC decomposition at T_{max} (temperature of maximum CO_2 concentrations) diminishes progressively with increasing HCl concentrations for lithified rock samples (i.e., 1207-GR-11 and MS05-135) (Fig. 2a and 2b), consistent with slightly broadening thermograms and elevations in standard deviations of activation energies (σ_E) (Table 2). Since T_{max} values are ~ 540 °C and ~ 600 °C for 1207-GR-11 and MS05-135, respectively, within the decomposition temperature window of heavily altered petrogenic OC, such decreases in peak CO_2 decomposition also indicate a reduction in the content of

225   thermochemically recalcitrant OC. In terms of other two samples, whereas no significant changes are seen in the sediment CJK A6-3 (Fig. 2c) along the HCl concentration gradient, a horizontal shift of thermograms towards lower temperatures has been observed for the sediment AREX R7 (Fig. 2d), suggestive of OC being thermochemically more labile as a consequence of

elevated HCl concentrations. With the exception of CJK A6-3, the uniform alteration of OC toward labile thermochemical properties, by lowering proportions of recalcitrant OC and/or shifting thermograms to lower temperatures, implies systematic

230 effects caused by HCl concentrations (Fig. 2).

change in
←→ thermal stability

Change in TOC
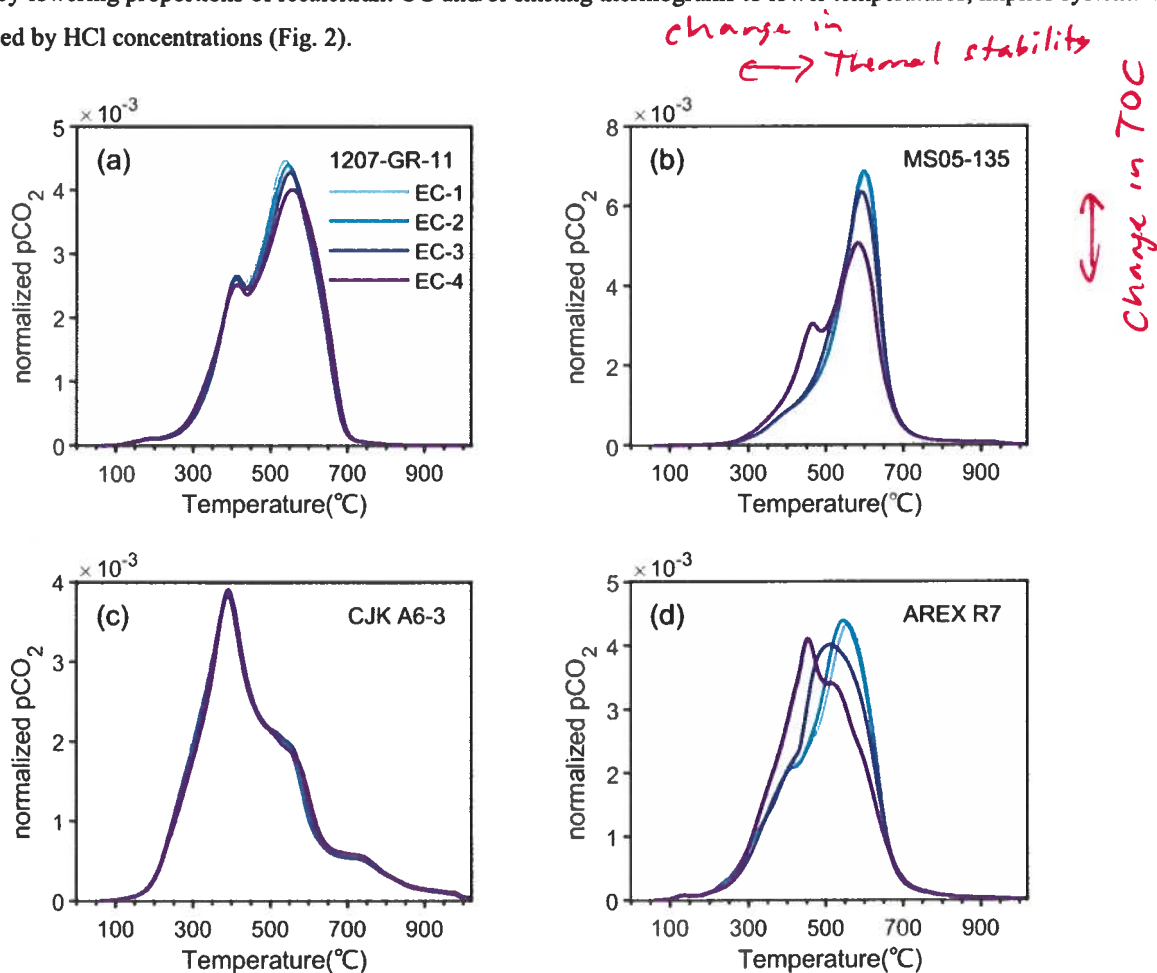
Fig 2: Normalized thermograms of subsamples rinsed with different concentrations of HCl. **(a)**, **(b)**, **(c)** and **(d)** are subsamples of 1207-GR-11, MS05-135, CJK A6-3 and AREX R7, respectively. See methods for the definition of EC-1 to EC-4.

235 Pronounced variations in thermograms and accordingly enhanced lability of OC rinsed with concentrated HCl are likely attributed to structure alteration of mineral matrices and their interactions with OC, in addition to leaching of a fraction of dissolvable OC through acid rinsing. In general, OC exists in sediments in the form of free molecules, aggregates, bound to minerals, or as kerogens. Considerable amount of OC in sediments is stabilized as OC-Fe chelates (Mackey and Zirino, 1994; Lalonde et al., 2012), coated onto mineral surfaces (Mayer, 1994a, b; Vogel et al., 2014), trapped in carbonate matrices (Ingalls

240 et al., 2004; Summons et al., 2013; Yang et al., 2025; Zeller et al., 2020; Zeller et al., 2024) and preserved in mineral interlayers

(Blattmann et al., 2019; Huang et al., 2023; Kennedy et al., 2002). The dissolution of carbonates under diluted HCl would release OC initially preserved in the carbonate matrix (Zeller et al., 2020), whereas other minerals and OC associated therein are undisturbed. Through the addition of HCl solution, a minimal proportion of OC is dissolved in the aqueous phase and washed away at the following water rinsing steps. In comparison, elevated concentrations of HCl would further attack other

245 minerals (e.g., iron oxides, clay minerals) and leach metal ions into solution (Brodie et al., 2011; Kumar et al., 1995). In fact, former studies demonstrated that concentrated acids cause metal isotopic fractionations by leaching minerals disproportionally (Fernandez and Borrok, 2009; Rongemaille et al., 2011). Such postulation is in consensus with elevated mass loss with concentrated HCl in this study (Table 2). On one hand, concentrated HCl promotes the leaching of OC by releasing and dissolving molecules initially associated with minerals. On the other hand, the destruction of mineral matrix induces profound

250 structural alterations of organic-inorganic complexes, and reduces organo-mineral binding energy, which is evidenced by shifts of some samples toward lower activation energies (Table 2). Therefore, patterns of thermograms and energy distributions coeval with variations in TOC contents, isotopic values and mass loss along the gradient of HCl concentrations (Table 2).

Discrepant responses to HCl also suggest that effects of acidification conditions are sample-specific and thus warrant a careful examination of sample properties. We propose that diverse responses of samples are primarily driven by organo-mineral

255 interactions and diagenetic alterations. Two lithified sediments, albeit with contrasting carbonate contents, respond similarly to elevated HCl concentrations (i.e., denudation in main peak height and broadening thermogram) without significant thermographic shifts. This is likely due to strong organo-mineral interactions established and homogenized OC properties with time. As diagenesis proceeds, processes including the breakdown of biopolymers, modification of functional groups and secondary condensation reactions take place successively (Burdige, 2007), leading to enhanced degrees of reconstruction and

260 lower overall vulnerability to external alterations.

In comparison, AREX R7 is a modern high-latitude surface sediment with limited diagenetic alteration and hydrodynamic sorting. Accordingly, the majority of OC is likely bound to minerals loosely, and thus would respond considerably to acid concentrations through reversibly breaking or reestablishing weak bonds, which is expressed as horizontal shifts of thermograms (Fig. 2). However, CJK A6-3 represents sediment deposited under the oxic setting on an expansive shelf after

265 extensive degradation along fluvial systems. Consequently, OC preserved therein, regardless of its terrestrial or marine origin, is strongly bond to minerals and thus exhibits sluggish responses to increasing HCl concentrations with nearly overlapping thermograms (Fig. 2) (Huang et al., 2023).

3.3 Thermographic distortion by acid fumigation and the effect of calcium chloride

Significant discrepancies are observed between acid fumigation and acid rinsing results (Fig. 3). To simplify potential variables

270 and to compare differences between acid fumigation and rinsing, we combined and averaged thermograms of acid rinsed subsamples. Direct comparison between acid fumigation and rinsing suggests that conventional acid fumigation (fume II) largely lowers or diversifies thermochemical stability of OC, which is possibly related to two mechanisms. On one hand, acid

fumigation establishes an ambient environment of vaporized HCl, which further attacks sample particles through formation of concentrated HCl solution. On the other hand, $CaCl_2$ forms after decarbonation further interacts with OC and alters the structure

275   of OC and organo-mineral interactions accordingly.
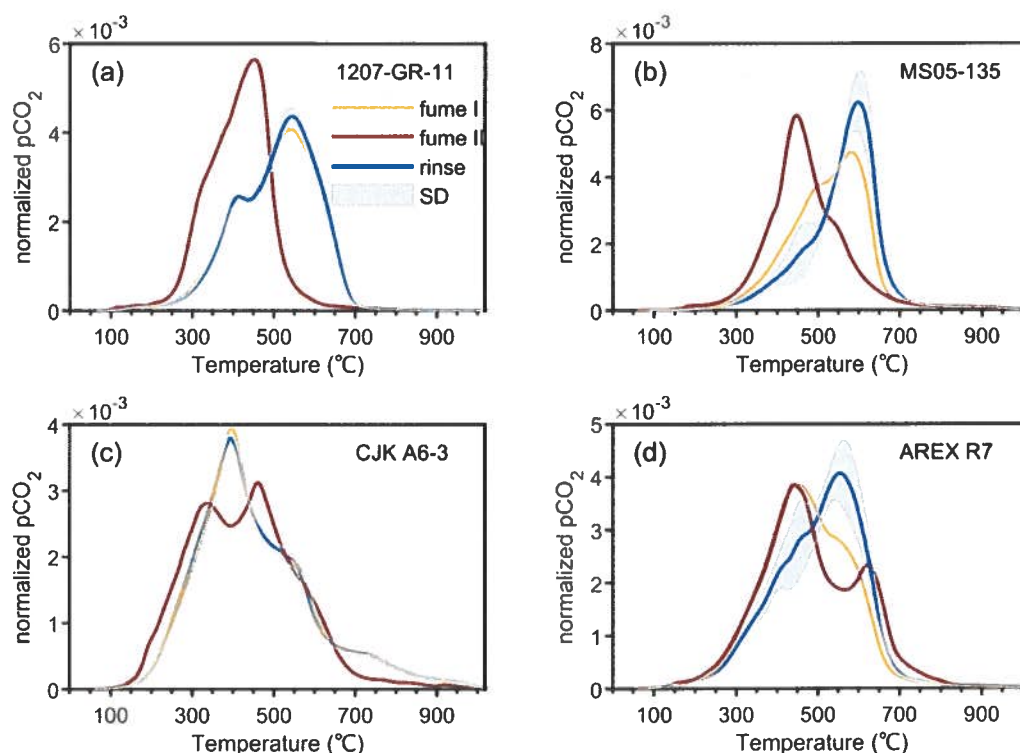
Fig 3: Normalized thermograms of subsamples after acid rinsing and fumigation. **(a)**, **(b)**, **(c)** and **(d)** represent subsamples of 1207-GR-11, MS05-135, CJK A6-3 and AREX R7, respectively. Yellow curves and dark brown curves stand for subsamples acidified by EC-11 (or fume I) and EC-12 (or fume II), whereas blue curves are mean values of EC-1 to EC-10 with shaded

280   intervals representative of standard deviations.

To unravel potential mechanisms of contrasting thermograms after acid fumigation, we first evaluate the impact of HCl concentration generated from acid vapor. To do so, we add an additional acid fumigation-rinsing control experiment (fume I), in which acid fumigated powders were further rinsed with Milli-Q water to remove $CaCl_2$. Results show that thermograms of

285   fume I subsamples are, in general, comparable to those of HCl rinsed subsamples and exhibit constant gradation following HCl concentrations (Fig. 3). Explicitly, thermographic patterns of fume I subsamples are consistent with results anticipated for concentrated HCl pretreatments (e.g., 12 N HCl). Therefore, it indicates that the concentrated HCl solution through the dissolution of HCl vapor exerts a noticeable and systematic impact on the thermochemical characteristics of sedimentary OC.

The contrasting difference between fume II and other water-rinsing experiments, including fume I as well as HCl rinsing,
290   suggests that CaCl₂ may play a dominant role in modifying thermochemical properties of sedimentary OC, given the residual
CaCl₂ being the main difference between fume II and others. We propose that CaCl₂ may influence thermograms in two distinct
ways. HCl or chlorine gas may boost the breakup of organo-mineral bonds or covalent bonds in OC and thus stimulate the
decomposition of OC at elevated temperature (Plante et al., 2013). In the meantime, it is noteworthy *in our system* that chlorine generated
by the decomposition of CaCl₂ under high temperatures also interacts directly with the catalytic wires (Hemingway et al.,
295   2017b), corrodes reactor tubes (Supplementary file Fig. 4), and thus, influences the reaction rates. Furthermore, calcium ions
(and other metal ions) may enhance organo-cation interactions or facilitate organo-mineral aggregations (Keil and Mayer,
2014; Rowley et al., 2018), and thus complicate reaction kinetics. It has been demonstrated that Ca^{2+} in soils and sediments
enhances the sorption and stabilization of OC (Feng et al., 2005; Rowley et al., 2018). However, the proposed Ca-stabilization
mechanism contradicts the observation of more labile nature of fume II subsamples. Therefore, it is possible that HCl and
300   chlorine gas, other than the calcium ion, play a more important role in affecting the ultimate thermochemical decomposition
of sedimentary OC after fumigation.

To further demonstrate the assumption of thermochemical biases induced by CaCl₂ (fume II), we carried out a CaCl₂ addition
experiment with the in-house standard (Irati T2). Under this experiment, one aliquot of Irati T2 was added with ~ 30mg CaCl₂
powders, whereas another aliquot of Irati T2 was added with ~ 30mg CaCl₂ powders, moistened with Milli-Q water, oven
305   dried, and then rinsed three times to remove chloride ions (part of Ca^{2+} and other cations co-precipitated with OC). The amount
of CaCl₂ added (~ 30mg) was carefully determined as it represents the median of potential CaCl₂ precipitates in four fume II
subsamples (~ 20mg to > 100 mg). Subsequently, two aliquots were successively analyzed for RPO and compared with results
of raw Irati T2 material (Fig. 4). Consistent with the assumption above, thermograms of raw Irati T2 and that with water rinsing
after addition of CaCl₂ resemble each other and are distinct from that with the addition of CaCl₂, but without water rinsing.
310   Therefore, it further demonstrates that thermographic distortion of fume II subsamples is most likely an artifact due to the
presence of CaCl₂. We further measured the raw Irati T2 material before and after the analyses of fume II subsamples, which
apparently corrodes and melts catalytic wires. Constant Irati T2 thermograms suggest that the corrosion of catalytic wires may
not exert an apparent influence on thermographic distortions (Supplementary file Fig. S1). However, it is noteworthy that the
CO₂ yield after the corrosion of catalytic wires declines significantly, likely due to the incompletely catalytic conversion of
315   CO to CO₂. Overall, the above results suggest that CaCl₂ biases the thermographic distortion by dictating the pyrolytic
breakdown of sedimentary OC.
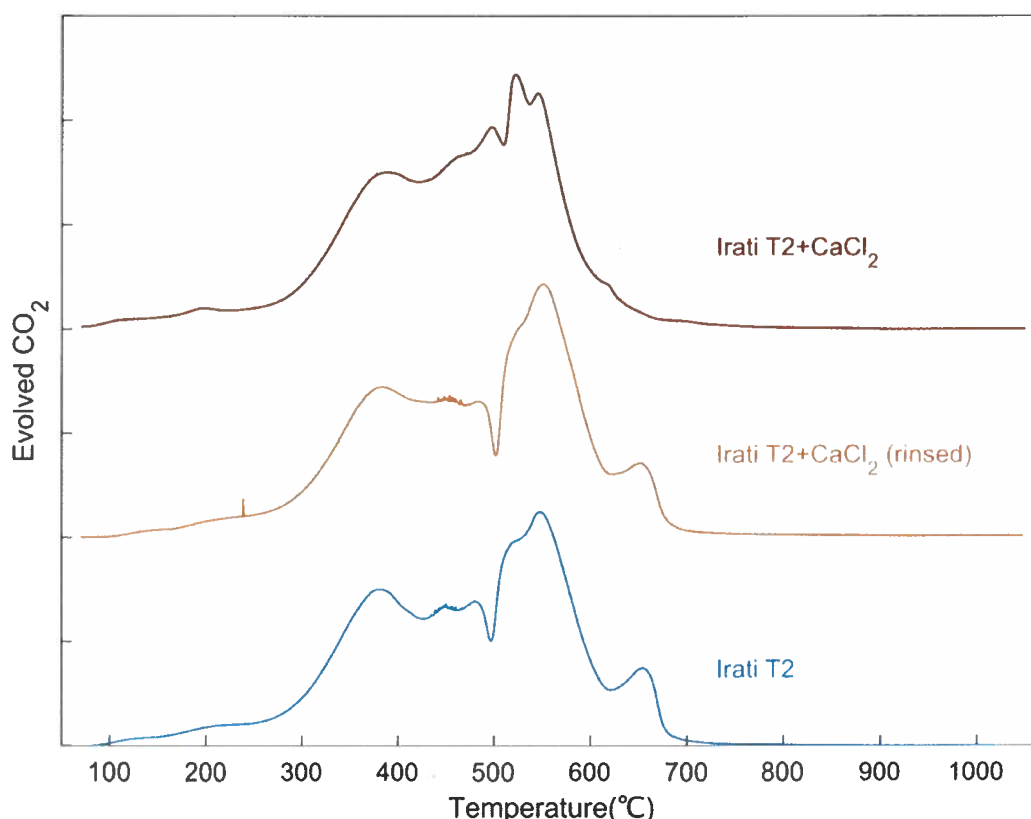
Fig 4: Parallel thermograms of the in-house standard (Irati T2) with distinct treatments. From bottom to top, the blue curve is Irati T2 without any extra treatment; the dark orange curve represents Irati T2 mixed with ~30 mg CaCl₂ and then rinsed with

320   Milli-Q water preceding RPO analysis; whereas the dark brown curve is Irati T2 with addition of ~30 mg CaCl₂ preceding RPO analysis. All samples were analyzed in sequence within two days to alleviate potential systematic biases with time.

3.4 Decarbonation pretreatments deviate thermochemical properties from pristine conditions

Given diverse responses of sediments to HCl concentrations and acid fumigation, it is reasonable to assume that all

325   pretreatment conditions would have resulted in noticeable deviation of sample properties away from pristine conditions held by unprocessed raw materials. To verify and examine the extent of deviations, we compared thermograms between acidified (i.e., rinsing versus fumigation) and unacidified subsamples. Due to the influence of IC in raw materials, thermograms of both processed and raw sediments were first normalized to back-calculated TOC content of each specific sample. As organic carbon contents of raw subsamples cannot be directly estimated, we used back-calculated TOC of fume II subsamples, which minimize

330   OC loss, to approximate those of raw subsamples. Former studies suggested that IC decomposition normally commences at about 500 °C or higher (Hemingway et al., 2017a; Capel et al., 2006). Thus, we only focus on thermographic segments evolved

under 450 °C, below which IC decomposition and consequential CO_2 production are considered to be negligible. Accordingly, we assume that any apparent inconformity of thermograms is ascribed to OC decomposition or alteration.

335   When overlain together, acid rinsed subsamples, with the exception of AREX R7, are, on average, more proximal to pristine conditions (Fig. 5). It is noteworthy that the magnitude of raw material thermograms may be overestimated, due to the potential decomposition of some carbonate minerals at lower temperatures (Hazra et al., 2022; Sebag et al., 2018) and/or OC loss during acid fumigation. Low-temperature-prone carbonates may reasonably explain the abnormality of AREX R7, of which the raw material features relatively low μ_E (182.48 kJ mol⁻¹; not shown) and T_{max} value (Supplementary file Fig. S5). Accordingly, we are confident to conclude that acid rinsing is more conducive to maintaining sediment pristine conditions, producing reliable

340   and consistent thermochemical results.
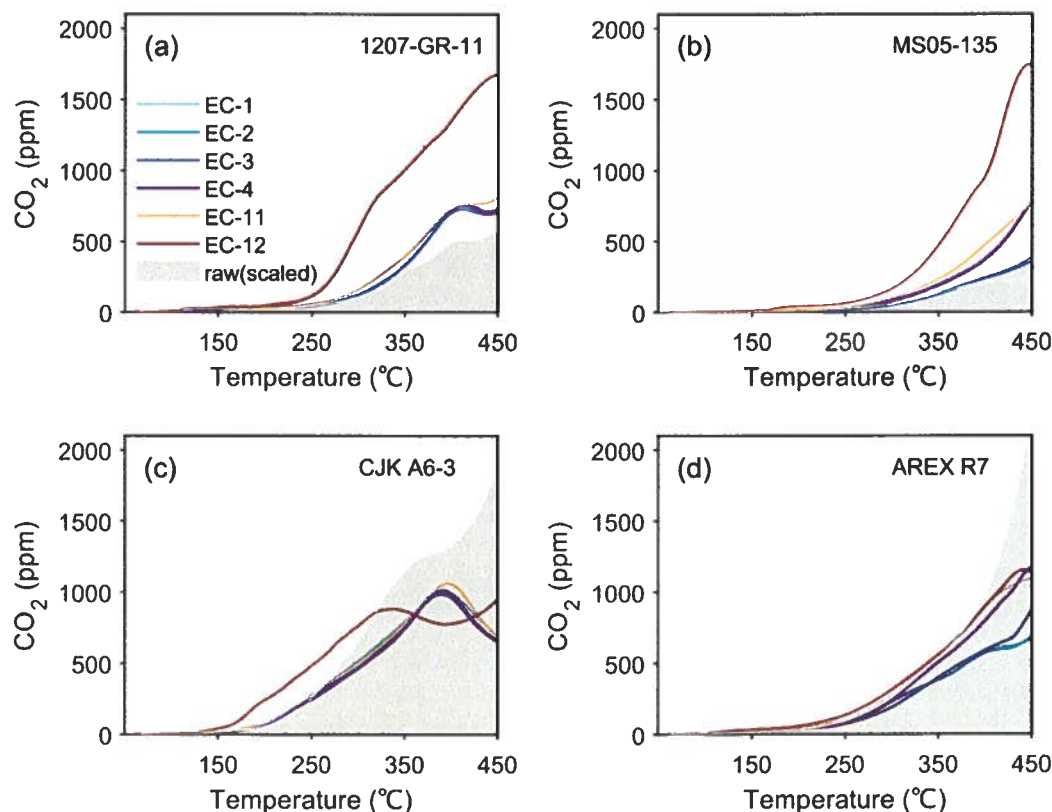
Fig 5: Evaluation of the proximity to the natural pristine states of subsamples acidified by different methods. **(a)**, **(b)**, **(c)**, and **(d)** are subsamples of 1207-GR-11, MS05-135, CJK A6-3, and AREX R7, respectively. Each curve represents the thermogram of a subsample acidified by corresponding procedures. The grey area in each subgraph is the thermogram of the raw

345   (unacidified) aliquot after normalization to OC contents.

4 Conclusion and recommendations

In this study, we systematically evaluated the effects of twelve different acidification pretreatments on decarbonation using four representative samples. Our results demonstrate that ~~the choice~~ between acid rinsing and fumigation, ~~as well as HCl~~

350 ~~concentrations during acid rinsing~~, are two critical factors influencing bulk OC and thermochemical properties. Higher HCl concentrations led to greater OC loss, likely due to mineral dissolution by concentrated HCl, which alters organo-mineral interaction and leaches soluble OC fractions. Furthermore, significant differences in thermochemical results were observed between acid rinsing and fumigation. Through simulation experiments with an in-house standard, we attribute these differences to corrosive impacts from CaCl$_2$ decomposition and alterations of thermochemical properties by strong acid vapor during acid

355 fumigation. Based on these findings, we recommend using diluted HCl for acid rinsing, as it minimizes perturbation to the pristine conditions of raw samples.

Given results from this study, we propose the following suggestions for future decarbonation pretreatments. First, acid fumigation of sediments in silver capsules is preferred for the measurements of bulk OC and δ^{13}C values. However, acid fumigation is not applicable to samples containing a considerable content of carbonates as it removes IC incompletely. Acid

360 rinsing with low concentrations of HCl induces minimal alteration to organo-mineral interactions and is the ideal decarbonation pretreatment preceding thermochemical (e.g., RPO, Rock-Eval, thermogravimetric analysis), spectral (e.g., Raman) and molecular (e.g., biomarker) analyses. In addition, to completely remove IC and to minimize OC loss, moderate reaction time (~12 h or overnight) and freeze-drying are recommended. However, it should be noticed that freeze-drier may ~~be an underlying~~ organic contamination ~~without thorough cleaning~~ (Jiang et al., 2023). Furthermore, operations to accelerate the decarbonation

365 process, like heating ~~and sonication (not verified in this study)~~, seemingly do not produce significant deviations. However, protein-rich samples may not be the case as heating may accelerate the hydrolysis of proteins and cause significant leaching of soluble OC. ~~Besides,~~ our study suggests that thermochemical analysis can be a powerful way to disentangle OC properties unresolvable by bulk parameters.

Data availability

370 All data needed to evaluate the conclusions is involved in this paper. The RPO dataset of this study can be accessible through DOI: 10.5281/zenodo.14825000 (He et al., 2025).

Author contribution

S.H. and X.C. designed the study; S.H. and H.Y. conducted the experiments; X.C. secured fundings; S.H. drafted the manuscript with contributions from all co-authors.